

## VIII. 14. Scientific Evaluation on Effects of Chiropractic Treatment, a Type of Manual Therapy, Using Magnetic Resonance Imaging (MRI) and Positron Emission Tomography (PET)

Ogura T.<sup>1</sup>, Tashiro M.<sup>1</sup>, Masud M.<sup>1</sup>, Watanuki S.<sup>1</sup>, Shibuya K.<sup>2</sup>,  
Itoh M.<sup>1</sup>, Yamaguchi K.<sup>1,3</sup>, Fukuda H.<sup>4</sup>, and Yanai K.<sup>1,2</sup>

<sup>1</sup>Division of Cyclotron Nuclear Medicine, Cyclotron and Radioisotope Center, Tohoku University

<sup>2</sup>Department of Pharmacology, Tohoku University Graduate School of Medicine

<sup>3</sup>Advanced Image Medical Center, Sendai Welfare Hospital

<sup>4</sup>Institute of Development, Aging and Cancer, Tohoku University

### Introduction

Chiropractic is one of the manipulative therapies initiated by Daniel David Palmer in 1895 in the United States, and its purpose has been thought to be “improving neurophysiological functions that lead to enhancing the ability of natural healing of the body by adjusting dysfunction of the joint called subluxation in the spine, pelvis, and extremity<sup>1)</sup>”. Currently, chiropractic is legislated in the U.S. and in over 20 other countries of the world. Chiropractic spinal manipulation (CSM) is considered as one of the main treatment techniques for neuro-muscular-skeletal problems, and its main complaints of the patient are neck pain, back pain and low back pain<sup>2)</sup>. The autonomic nervous system (ANS) is also thought to be one of the areas influenced by CSM<sup>3,4)</sup>.

Despite clinical evidences for benefits of the spinal manipulation and apparent wide usage of it, physiological mechanisms underlying the effects of CSM are not clearly known<sup>5,6)</sup>. Although many studies on chiropractic have been performed all over the world, no study has been conducted to evaluate effects of one CSM treatment utilizing MRI and PET analyses. The aim of the present study is to investigate effects of one CSM in the treated peripheral structures and in the central nervous system (CNS)<sup>6)</sup>.

### Methods

For the MRI investigation, twenty low back pain patients (mean age: 28.0 y.o.) were divided into three groups, normal group, sacral base (SB) anterior group and SB

posterior group, by the pressure testing in Activator Methods (AM), one of chiropractic techniques, and the subjects received chiropractic treatment depending on the results of the pressure testing. T2 weighted sagittal lumbo-sacral MRI images were taken on subjects before and after the treatment, and measurements on the images were compared. The measurements included angles of sacral base (SBA), L5-S1 disc (LSDA), and lumbar lordosis (LLA) (Fig. 1)<sup>7)</sup>. The values were statistically analyzed by paired *t*-test. The present MRI study was approved by the Ethics Committee of Sendai Welfare Hospital.

For the present study, healthy male volunteers were recruited by putting up a poster in the campus of Tohoku University. Inclusion criterion was 1) men of 20 to 40 years old with the presence of cervical pain and shoulder stiffness, but without experience of receiving any types of manipulative treatment for at least one month prior to the experiment. Exclusion criteria were 1) the presence of disc problems such as disc herniation and significant disc degeneration, and 2) any other physical and mental disorders and medication that might affect brain function or perfusion. After giving informed consent, all 15 candidates were first assigned for MRI examination of the cervical region, and 3 subjects with disc problems were excluded from the study. Medical screening was also performed to confirm absence of any apparent disorders and medication that might affect brain function. In result, 12 male volunteers aged 21 to 40 (mean age  $\pm$  S.D.: 28.0 $\pm$ 6.8) were recruited into this study.

The present study was conducted in cross-over study design, in which each subject was examined twice (once in the "treatment" and the other time in the "control" conditions) in purpose of comparing the resting regional brain activity in the two conditions. In the treatment condition, subjects received a single CSM intervention, taking for around 20 minutes including a diagnostic procedure. And shortly after the CSM treatment, FDG-containing saline solution was injected to the subject through the left cubital vein (37 MBq) in a quiet room with the dim light. Subjects were asked to sit in a relaxed mood with their eyes closed for 30 min before scanning. The brain scan of the subject was initiated after 30 min of FDG injection, using a PET scanner, SET2400W (Shimadzu Inc., Kyoto, Japan). The PET scanning covered the entire brain in one scan, taking 10 minutes for emission scan, and another 5 min or so for transmission scan for tissue attenuation correction. In the other scan in the control condition, FDG was injected to the subject after a 20-min-long resting phase instead of CSM intervention. The following procedure was identical to the treatment condition. The radiation exposure due to one PET scan in this

study was estimated to be approximately 0.9 mSv<sup>6</sup>).

In addition, the order of these two scans, that is, “control – treatment” and “treatment – control”, was counter-balanced to minimize an “order effect”. The meaning of this order effect is that the study subjects tend to feel psychophysiological stress more in the first scan than in the second and following scans. Therefore, the protocol was prepared to minimize this order-associated effect. In result, the first scan was performed in the treatment condition in half of the subjects, and vice versa. And, the interval between the first and second scans was set to be at least 1 week in order to eliminate residual effect of treatment. The interval ranged from 1 to 6 weeks (mean interval  $\pm$  S.D.:  $22.4 \pm 12.5$  days). CSM was performed by the same chiropractor, an advanced proficiency rated doctor of Activator Methods (AM)<sup>6</sup>.

PET brain images were analyzed to identify regional changes in glucose metabolic rate using a software package, Statistical Parametric Mapping (SPM2, Functional Imaging Laboratory, London, UK). Positional errors between the 2 scans were corrected for each subject, using realignment function of SPM2. An FDG brain template distributed by Montreal Neurological Institute, McGill University, Canada, was used for anatomical standardization (spatial normalization) of the PET images by applying linear and non-linear transformations, by minimizing the inter-subject differences in gyral and functional anatomy. The normalized data were smoothed using isotropic Gaussian kernel of 12 mm (for x,y,z axes) to increase the signal-to-noise ratio by suppressing high frequency noise in the images<sup>6</sup>.

Voxel-by-voxel analysis such as SPM is the standard tool in detecting regional changes in radioactivity levels in certain brain regions. The most popular contrast in these studies has been to contrast “resting” with “task or stimulus”. For statistical analysis, all “voxel” values were normalized to an arbitrary global mean value of 50 mg/100 ml/min by ANCOVA to exclude the effects of inter-subject variability in global cerebral glucose metabolism. Paired t-test was applied to each voxel; only voxel clusters were maintained with voxels corresponding to  $p < 0.001$  in a single test and a cluster size of 10 voxel minimum in two ways. The statistical significance of a regional metabolic change was given in Z scores. The Z-value is the amount of difference between the target group mean value (the treatment condition, in this study) and the control mean value, divided by standard deviation of the control values  $[(\text{Mean}_{\text{target}} - \text{Mean}_{\text{control}}) / \text{SD}_{\text{control}}]$ . Empirically in SPM analysis, a Z score higher than 3.0 (approximately corresponding to  $p < 0.001$ ) is

roughly considered as statistically significant. The location of each statistical peak was identified based on a co-planar stereotaxic atlas of the human brain. Statistically significant areas were superimposed on the standard MRI brain template images (Fig. 2)<sup>6</sup>.

## Results

In the MRI analysis, nine subjects were classified into the SB anterior group, and 11 subjects were classified into the SB posterior group in this study. No subject was divided into the normal group in the present study. Apparent angle changes were observed between pre- and post-CSM MRI images in both groups. In the SB Anterior group, SBA was decreased in 8 subjects on the post-CSM MRI images except for one subject who showed a slight increase in the angle (Table 1). Decrease in both LSDA and LLA were observed in all 9 subjects (Table 1). In SB Posterior group, increasing of SBA was seen in 10 subjects, and no change was seen on one subject on the post-CSM MRI images (Table 1). Increased LSDA and LLA were observed in all 11 subjects (Table 1).

FDG-PET analysis revealed significant changes in regional cerebral metabolism between resting and treatment conditions. Increased glucose metabolism was observed in the inferior prefrontal cortex (BA 47), perigenual anterior cingulate cortex (BA 32), and middle temporal gyrus (BA 21) whereas decreased glucose metabolism was observed in the cerebellar vermis and visual association cortex (BA 19) in the treatment condition with comparison to resting condition (Fig. 2, Table 2)<sup>6</sup>.

Subjective and objective measures indicated significant differences. SRS-18 scores were significantly lower in the treatment condition ( $p < 0.01$ ), and VAS was also lower after CSM ( $p < 0.001$ ). Measurements of cervical muscle tone revealed significant differences after CSM (right:  $p < 0.002$ , left:  $p < 0.001$ ). Reduced salivary amylase values were also observed in treatment condition ( $p < 0.02$ )<sup>6</sup>.

Brain regions with metabolic increase in the treatment condition, and the regions with metabolic reduction in the treatment condition (Table 2 and Fig. 2). Both figures demonstrate results of voxel-by-voxel comparison of regional brain glucose metabolic images using statistical parametric mapping (SPM) (height threshold:  $p < 0.001$ , extent threshold: 10 voxel minimum)<sup>6</sup>.

## Discussion

Results of the MRI study indicated apparent changes of measurements on the

post-CSM MRI images compared to pre-CSM MRI images; however, two subjects did not show same kinds of changes on SBA measurement. One subject showed slightly increased angle in SB Anterior group, and the other indicated no change of the angle in SB Posterior group while measurements of LSDA and LLA on these two subjects showed same kinds of changes as others. It is clearly demonstrated that this phenomenon is caused by balancing effect of CSM on the alignment of the lumbar spine and the sacrum.

The measurements of SBA and LLA after CSM in this study were lower relative to the average value (SBS: 41.0/±7.0 degree) or normal range (LLA: 50~60 degree) of those angles in an article. These differences seem to be caused by recumbent position of the subject during imaging. Yochum and Rowe stated that the value of average SBA increases from recumbent to the upright position by 8 to 12 degree<sup>7)</sup>. Additionally, Andreasen et al. indicated that it is possible to reproduce the lumbar lordosis in the supine position by positioning the patient supine with straightened lower extremities<sup>8)</sup>. Beattie et al. reported a mean difference between the flexed and straightened lower extremities in the supine position are 12.2 degree<sup>9)</sup>. Therefore, the mean values of LLA after CSM in this study are within or close to the normal ranges of SBA and LLA.

In the present study, the most significant change was detected in the cerebellar vermis, which was deactivated in the treatment condition compared to the resting condition. The cerebellar vermis is considered to be playing a role in pain perception. Neuroimaging studies revealed a pattern in the cerebellar activation during pain response<sup>10)</sup>. In addition, the cerebellar vermis is thought to be involved with the autonomic nervous system<sup>10)</sup>. Thus, deactivation of the cerebellar vermis may be related to pain reduction and reduced sympathetic tone in this study<sup>6)</sup>. The perigenual anterior cingulate cortex, inferior prefrontal cortex, and middle temporal gyrus were activated in the treatment condition in the present study. The cingulate cortex and inferior prefrontal cortex are known to be involved in the generation of autonomic responses<sup>11)</sup>. Thus, the results of the present study suggest that activation of the perigenual anterior cingulate cortex and inferior prefrontal cortex may arise from sympathetic relaxation. In conclusion, the present study might demonstrate effects of one CSM in the treated peripheral structures and in CNS. Further neuroimaging studies are needed on effects of CSM<sup>6)</sup>.

## References

- 1) Jansen J., Chiropractic Theory, Application, and Practice. Kagaku-shinbunsha: (1969) 3.
- 2) World health organization Kobe Centre. Traditional Medicine, Annual Report (2004) 24.
- 3) Budgell B.S., J. manipulative Physiol. Ther. **23** (2000) 104.
- 4) Slosberg M., J. manipulative Physiol. Ther. **11** (1988) 181.
- 5) Picker J.G., Spine J. Sep-Oct **2**(5) (2002) 357.
- 6) Ogura T., Tashiro M., Masud M., Watanuki S., Shibuya K., Yamaguchi K., Itoh M., Fukuda H., Yanai K., Regional cerebral metabolic changes in patients with neck pain following chiropractic spinal manipulation: [<sup>18</sup>F]FDG PET Analysis. Alternative Therapies in Health and Medicine (in press).
- 7) Yochum T.R., Rowe L.J., Essentials of Skeletal Radiology. Second Ed. Williams and Wilkins (1996) 159.
- 8) Andreasen M.L., Langhoff L., Jensen T.S., et al., J. Manipulative Physiol. Ther. **30** (2007) 26.
- 9) Beattie P.F., Brooks W.M., Rothstein J.M., et al., Spine **19** (1994) 2096.
- 10) Sacchetti B., Scelfo B., Strata P., Neuroscience **162** (2009) 756.
- 11) Schlindwein P., Buchholz H.G., Schreckenberger M., et al., Autonomic Neuroscience **143** (2008) 27.

Table 1. Comparisons of angles between before and after CSM.

	Group	Before Mean (SD)	After Mean (SD)	P Value
SBA	SB A	39.2 (+/-4.9)	35.3 (+/-4.9)	p=0.001
	SB P	31.3 (+/-3.8)	35.0 (+/-3.9)	p=0.0001
LSDA	SB A	16.0 (+/-3.5)	11.5 (+/-3.7)	p=0.001
	SB P	12.7 (+/-2.8)	16.0 (+/-2.9)	p=0.001
LLA	SB A	45.7 (+/-4.9)	38.9 (+/-5.2)	p=0.001
	SB P	37.0 (+/-3.7)	41.9 (+/-5.2)	p=0.000001

Abbreviations: SBA=Sacral Base Angle, LSDA=L5-S1 Disc Angle, LLA=Lumbar Lordosis Angle, SB A=Sacral Base Anterior, SB P= Sacral Base Posterior, SD=Standard Deviation.

Table 2. Activation/Deactivation areas after CSM.

	Anatomical Region	coordinates x,y,z (mm)	Brodmann Area (BA)	Z score
Activation	IPC	54 24 -8	47	3.82
	MTG	-48 -36 0	21	3.73
Deactivation	PACC	22 24 38	32	3.48
	CV	4 -42 -18		4.62
	VAC	4 -90 24	19	3.64

Abbreviations: IPC=Inferior Prefrontal Cortex, MTG=Middle Temporal Gyrus, PACC=PACC=Perigenual Anterior Cingulate Cortex, CV=Cerebellar Vermis,VAC=Visual Association Cortex.



Figure 1. Angle measurements on MRI images. Sacral Base Angle (LEFT), L5-S1DiscAngle (MIDDLE), Lumbar Lordosis Angle (RIGHT)

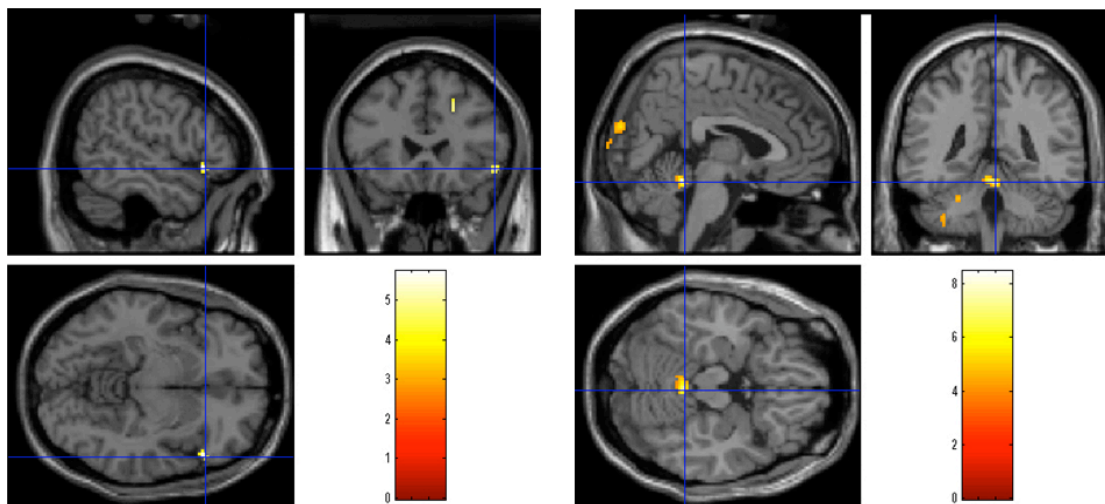


Figure 2. Results of FDG-PET Analysis Regional activation (Left) and deactivation (Right) due to chiropractic spinal manipulation. Brain regions showing a metabolic increase (Left) and a metabolic reduction (Right) in the treatment condition. Both figures demonstrate results of voxel-by-voxel comparison of regional cerebral glucose metabolic images using statistical parametric mapping (SPM) (height threshold:  $p < 0.001$ , extent threshold: 10 voxel minimum).